ANALYSIS OF THE DISCHARGE COEFFICIENT OF A SPRING LOADED PRESSURE RELIEF VALVES DURING ITS DYNAMIC BEHAVIOR

A. J. Ortega, arturo@simdut.com.br
B. N. Azevedo, bruno_n_azevedo@aluno.puc-rio.br
L. F. G. Pires, lpires@simdut.com.br
A. O. Nieckele, nieckele@puc-rio.br
Pipeline Thermo-Hydraulic Simulation Group – Mechanical Engineering Department – PUC/Rio
Rua Marques de São Vicente 225 – Gávea, CEP 22453-900, Rio de Janeiro, RJ, Brazil.

Abstract. *Direct acting spring loaded pressure relief valve is one of the most important devices to ensure security to pipeline oil transport. However, relief valves' manufactures generally only provide information on valve characteristics under full opening stage, which is obtained under steady state regime, therefore, valve and flow's transient behavior are neglected. Understanding the transient behavior of relief valves is crucial because critical conditions may be attained, damaging the pipeline. In order to overcome this lack of information, a direct acting spring loaded pressure relief valve's computational model was developed. A simplified two dimension model was built based on the valve geometrical and constructive characteristics. Further, a dynamic equation, which defines the valve disc position, was implemented. From the solution of the transient form of the conservation equations, the velocity and pressure distributions were obtained, allowing the determination of the discharge coefficient versus valve opening under its transient state. Comparisons with one-dimensional integral approach model were performed to evaluate the model.*

Keywords*: Pressure relief valve, dynamic characteristics, discharge coefficient, incompressible flow, computational simulation*

1. INTRODUCTION

Relief and safety valves are fundamental equipments for oil and gas pipelines and load/unload terminals. The installation integrity and workers safety depend on the appropriate design and performance of these equipments. In spite of the importance of relief valves, there is lack of information about the dynamic behavior of these equipments. Thus, users are forced to work using valve characteristics supplied only by manufacturers. Further, the information supplied by them is generally restricted to situations of maximum discharge flow. Data about the full dynamic behavior of the relief valves during their opening stage, which is fundamental for analysis of transients during their actuation, is usually not available.

In spite of the importance of relief valves, only a few works about its dynamic behavior has been published. Catalani (1984) performed a dynamic stability analysis of a relief valve and identified the effects of its components on its stability. The undesired phenomenon named *chatter* (abrupt oscillations of the valve disc) was studied by MacLeod (1985) who modeled, using differential equations, the dynamic of a relief valve and identified the conditions to avoid it. In 1991 Shing made a study about the dynamic and static characteristics of a two stage pilot relief valve, determined the governing parameters of the valve response and presented recommendations in order to improve them. The dynamic of a direct operated relief valve with directional damping was studied by Dasgupta et al (2002) using the *bondgraph* technique. Maiti et al (2002) studied the dynamic characteristics of a two-stage pressure relief valve with proportional solenoid control of its pilot stage. According to their results, the overall dynamic behavior is dominated by the solenoid characteristic which is related to a applied voltage. Boccardi et al (2005) analyzed experimentally the water/vapor two phase flow through a relief valve. A new correlation for the discharge coefficient was developed, by comparing the experimental data with the solution of the flow based on a homogeneous model. Ortega et al (2008a) presented a work where the discharge coefficient of a pressure relief valve was determined numerically for different static positions of the valve disc. The flow was simulated using a two-dimensional, axis-symmetric model, as well as, employing $\kappa-\varepsilon$ and $\kappa-\omega$ SST turbulent models. In the same year, Ortega et al (2008b) developed a mathematical model of a direct acting pressure relief valve. Its governing parameters were identified and a sensibility analysis was carried out in order to determine its influence.

The objective of this work is to analyze the discharge coefficient of a direct acting spring loaded pressure relief valve (*PRV*) based on the dynamic actuation of a *PRV* two-dimensional dynamic model. The resulting flow behavior is evaluated by comparing with the solution obtained with a *PRV* one-dimensional dynamic model. In this last model, the discharge coefficient was previously determined based on the static behavior of the *PRV* disc.

2. MATHEMATICAL MODEL

Although the dynamic behavior of a *PRV* is strongly influenced by its geometric configuration and dimensions, a simplified geometry, as shown in Fig. 1, was considered as to a first prototype to develop the mathematical model. The

simplified system is composed of a spring, a cap or disc and an input flow pipe (valve wall). For the flow analysis through the *PRV*, the fluid was considered incompressible and isothermal. Also, due to the cylindrical shape of the geometry, the flow was considered axis-symmetric.

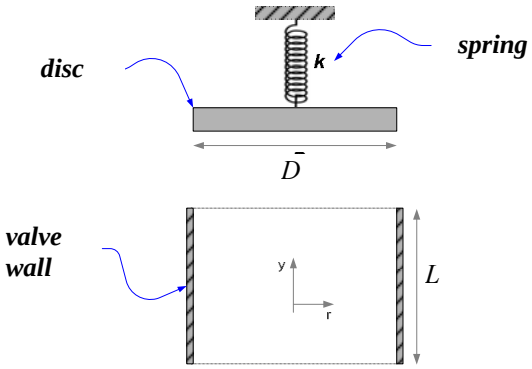

Figure 1 – *PRV* simplified system

2.1. One-dimensional Integral Model

The *PRV* starts opening when the operation pressure P_a exceeds the set point pressure P_{sp}. During the valve disc displacement, the Newton's second law can be applied to the valve disc as illustrated in Fig. 2, resulting in the spring-disc dynamic system equation, Eq. (1).

$$F_f - k(Y_D + Y_o) - c\frac{dY_D}{dt} - m_D g - P_o A = m_D \frac{d^2 Y_D}{dt^2}, \tag{1}$$

where F_f is the force applied by fluid to valve disc , k is the spring constant, Y_D is the valve disc displacement, Y_o is the spring initial deformation, c is the spring viscous damping coefficient, m_D is the disc mass, g is the gravity acceleration, P_o is the external pressure (atmospheric pressure) and A is inlet pipe cross section and disc area.

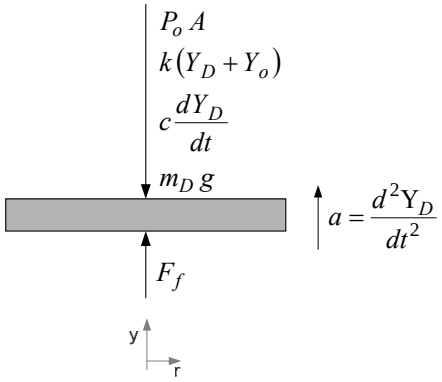

Figure 2 – The valve disc free body diagram during its displacement

Applying the principle of conservation of linear momentum in the y direction to control volume inside the *PRV* illustrated in Fig. 3, neglecting the time y momentum variation inside the control volume, since it can be considered small in relation to the others quantities, it results in

$$\sum F_y = \frac{\partial}{\partial t}\int_{CV} u_y \, \rho \, d\forall + \int_{CS} u_y \, \rho \, \vec{u} \bullet d\vec{A} \;\Rightarrow -\rho g A(L + Y_D) - F_f + P_a A = -u_e \rho u_e A, \tag{2}$$

where ρ is the fluid density, L is the length of the valve wall, F_f is the reaction applied by the valve disc to fluid, u_e is the inlet average velocity and P_a is the operation pressure or the *PRV* input pressure.

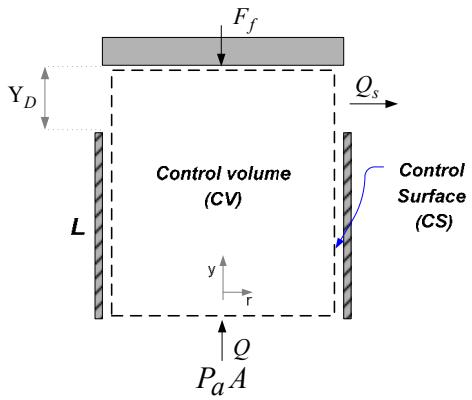

Figure 3 – Control volume inside of the *PRV* during its actuation

Combining the spring-disc dynamic equation, Eq. (1), with the fluid momentum conservation equation, Eq. (2), the following expression is obtained

$$0 = m_D \frac{d^2 Y_D}{dt^2} + c \frac{dY_D}{dt} + (k + \rho g A) Y_D + k Y_o + \rho g A L + m_D g - (P_a - P_o) A - Q^2 \frac{\rho}{A}, \tag{3}$$

where $Q = \rho u_e A$ is the average flow rate coming into the control volume.

Initially the valve is closed (Y_D=0, dY_D/dt=0), and it will only open when the operation pressure P_a is superior to the set point pressure P_{sp}. Therefore, the initial spring deformation Y_o is adjusted to attend this condition, and it can be determined from Eq. (3) as

$$Y_o = \frac{1}{k}\left[(P_{sp} - P_o) A - \rho g A L - m_D g\right]. \tag{4}$$

where P_{sp} is the set point pressure.

Equating (3) can be simplified by substituting the initial spring deformation expression, Eq. (4), resulting in

$$0 = m_D \frac{d^2 Y_D}{dt^2} + c \frac{dY_D}{dt} + (k + \rho g A) Y_D - (P_a - P_{sp}) A - Q^2 \frac{\rho}{A}. \tag{5}$$

Applying the principle of mass conservation into the *PRV* control volume during its actuation, Fig. 3, the flow rate leaving the control volume Q_s can be related to the inflow rate Q and the valve disc displacement Y_D as

$$0 = \frac{\partial}{\partial t} \int_{CV} \rho \, d\forall + \int_{SS} \rho \, \vec{u} \bullet d\vec{A} \quad \Rightarrow \quad 0 = A \frac{dY_D}{dt} - Q + Q_s, \tag{6}$$

Further, the valve outflow rate Q_s can be defined by the valve equation as

$$Q_s = C_d A \sqrt{2 \frac{(P_a - P_o)}{\rho}}, \tag{7}$$

where C_d is the discharge coefficient and A is a reference area, which, in this work, was considered as the valve disc area.

Finally, the equation that governs the dynamic behavior of the *PRV* during its actuation can be obtained by combining Eqs. (7), (6) and (5) as

$$\begin{aligned} 0 = {} & m_D \frac{d^2 Y_D}{dt^2} + \left(c - 2 C_d A \sqrt{2\rho(P_a - P_o)}\right) \frac{dY_D}{dt} + \\ & + (k + \rho g A) Y_D - (P_a - P_{sp}) A - \left(\frac{dY_D}{dt}\right)^2 \rho A - 2 C_d{}^2 A (P_a - P_o) \end{aligned} \tag{8}$$

Equation (8) was solved numerically using a fourth-order *Runge-Kutta* method. As initial condition the *PRV* was considered closed. At the valve inlet, a constant total pressure was imposed, in other words, the sum of the dynamic with static pressure were taken as constant during time evolution. The flow was discharged to ambient at atmospheric pressure. The numerical algorithm was implemented using *Fortran*, and details can be found in Ortega et al (2008).

2.1.1 Discharge Coefficient

The discharge coefficient C_d is one of the most critical parameter to be specified. It depends on the flow distribution inside the valve. Usually, it is determined experimentally, based on steady state flow with different valve openings.

For the one-dimensional model, the discharge coefficient, C_d, was determined numerically (Ortega et al, 2008a), considering a steady state regime for different valve openings, as it is done experimentally. This parameter was established from the flow field inside the simplified valve, illustrated in Fig. 1, employing the software FLUENT, with the following dimensions: L = 0.2 m, D = 0.1m and Y_{Dmax} = 0.1 m. The valve was considered axis-symmetric, therefore, several 2D turbulent steady state flow were obtained, for different valve openings, through the solution of the Reynolds-averaged mass and momentum equations (RANS). The turbulent viscosity was determined with the κ–ω SST model (Menter, 1994), which was developed to blends the effectively robust and accurate formulation of the standard κ–ω model in the near-wall region with the free-stream independence of the κ–ε model in the far field. The blending is designed to be one in the near-wall region, which activates the standard κ–ω model, and zero away from the surface, which activates the transformed κ–ε model.

The turbulent eddy viscosity μ_t is defined as

$$\mu_t = \rho \frac{k}{\omega\ \varepsilon} \tag{9}$$

where ω is the specific dissipation, and ξ is the blending term. There is also a cross-diffusion term D_ω included to the ω equation. The model requires the solution of two conservation equations, one is the standard κ equation, and the other is specific dissipation ω equation. These equations are given as

$$\mathbf{div}\,(\rho \vec{V}\,\kappa) = \mathbf{div}\,[(\mu + \mu_t / \sigma_\kappa)\,\mathbf{grad}\quad \kappa] + G_\kappa - Y_\kappa \tag{10}$$

$$\mathbf{div}\,(\rho \vec{V}\,\omega) = \mathbf{div}\,[(\mu + \mu_t / \sigma_\omega)\,\mathbf{grad}\quad \omega] + P_\omega - Y_\omega \tag{11}$$

where G_κ represents the production of turbulent kinetic energy due to mean gradients, while G_ω is the production of ω. Y_κ and Y_ω are the destruction of κ and ω, due to turbulence. The model is presented in detail in *FLUENT,* v6.3 (2008).

A operating pressure, P_a, of 2 atm was set at the inlet and the discharge pressure P_o was set as 1 atm. Water was selected as the working fluid (ρ = 1000 kg/m^3 and μ= 10^{-3} Pa-s). From the converged flow field, the discharge coefficient C_d was calculated using Eq. (7). Figure 4 presents the discharge coefficient C_d as a function of the different opening, normalized by the maximum aperture $Y_{D\mathbf{max}}$ (Y'_D=Y_D/$Y_{D\mathbf{max}}$). At the same figure, a third order polynomial adjusted to fit the data was plotted. This polynomial was included in Eq. (8) to determine the dynamic valve behavior.

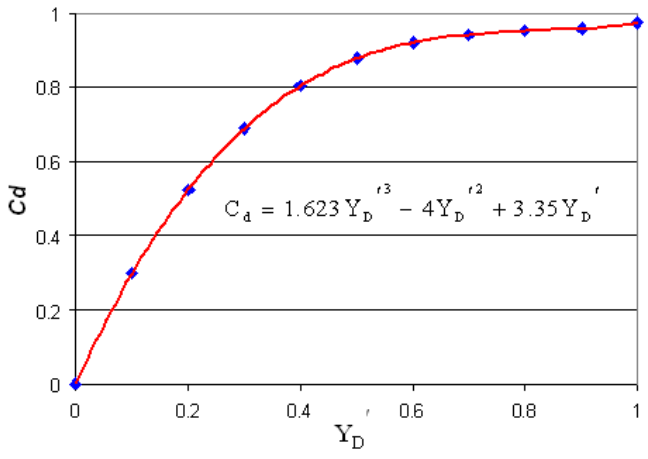

Figure 4 – Discharge coefficient calculated numerically

2.2. Two-dimensional Dynamic Model

The *PRV* dynamic behavior was obtained by employing the software FLUENT 6.3.26 (2006). An implicit, unsteady, two-dimensional (axis-symmetric) model was built. Additionally, at each time step, the valve disc position was determined by the solution of the spring-disc dynamic system equation, Eq. (1), which was implemented in *C* programming language and coupled with FLUENT as a user defined function, *UDF*.

The turbulent velocity and pressure fields were determined by the solution of the transient Reynolds average conservation equations of mass and momentum, coupled with a turbulence model:

$$\mathbf{div}\ (\vec{V}) = 0 \tag{12}$$

$$\partial(\rho\,\vec{V})/\partial t + \mathbf{div}\ (\rho\,\vec{V}\,\vec{V}) = \mathbf{grad}\ P + \mathbf{div}\ \{(\mu+\mu_t)[\mathbf{grad}\ \vec{V} + (\mathbf{grad}\ \vec{V})^T]\} \tag{13}$$

where ρ is density, μ and μ_t are the molecular and turbulent viscosity, P is the pressure and $\vec{V}$ is the velocity vector.

The turbulence model selected was the traditional κ–ε model (Launder e Spalding, 1974) with standard wall functions. The details of this model are presented in FLUENT 6.3.26 (2008) documentation. The κ–ε turbulence viscosity is:

$$\mu_t = C_\mu\ \rho\,\frac{\kappa^2}{\varepsilon} \tag{14}$$

where C_μ=0.09 is a empirical constant, κ is the turbulent kinetic energy and ε is the dissipation rate. This model requires the solution of following two conservation equations for κ and ε.

$$\partial(\rho\,\kappa)/\partial t + \mathbf{div}\ (\rho\,\vec{V}\,\kappa) = \mathbf{div}\ [(\mu+\mu_t/\sigma_\kappa)\,\mathbf{grad}\ \ \kappa] + P_\kappa - \rho\,\varepsilon \tag{15}$$

$$\partial(\rho\,\varepsilon)/\partial t + \mathbf{div}\ (\rho\,\vec{V}\,\varepsilon) = \mathbf{grad}\ P + \mathbf{div}\ [(\mu+\mu_t/\sigma_\varepsilon)\,\mathbf{grad}\ \ \varepsilon] + c_{1\varepsilon}\ P_\kappa - c_{2\varepsilon}\ \rho\,\varepsilon\,\frac{\varepsilon}{\kappa} \tag{16}$$

where P_κ is the production of turbulent kinetic energy,

$$P_\kappa = \mu_t[\mathbf{grad}\ \vec{V} + (\mathbf{grad}\ \vec{V})^T] : \mathbf{grad}\ \vec{V} \tag{17}$$

and the empirical constants are $c_{1\varepsilon} = 1.44$; $c_{2\varepsilon} = 1.92$; $\sigma_\kappa = 1.0$ and $\sigma_\varepsilon = 1.3$.

The same boundary conditions as defined for the one-dimensional model was prescribed, i.e., no slip at the wall, constant total pressure at the valve inlet, and constant atmospheric static pressure at the outlet. The turbulent intensity at the valve inlet section was set as 10% with a characteristic scale equal to the valve diameter. In the case of a reverse flow at the valve exit, a backflow turbulent intensity of 1%, with a length scale of 10 mm were set.

The Figure 5a illustrates the grid of 30 x 110 nodes uniformly distributed. The method *PISO* (Issa, 1986) was employed for solving the pressure-velocity coupling. The equations were discretized with a second order upwind interpolation scheme.

(a) Grid distribution (b) Streamline

Figure 5 – Two-dimensional valve model. (a) Grid distribution (b) Streamline at a particular time step

Figure 6 illustrates schematically the sequence of the *PRV* process at different time instants, where it can be seen that the valve disc is positioned at different locations as determined by the spring-disc dynamic equation, Eq. (1).

The discharge coefficient C_d was determined from the two-dimensional dynamic model in a similar way as it was done for the static model, i.e. using Eq. (7). The transient solution was obtained as a consequent of the valve disc dynamic behavior governed by the spring-disc dynamic equation, Eq. (1). Figure 5b illustrates the streamlines for a particular time instant, where it can be seen the streamline curvature going in direction to the valve exit.

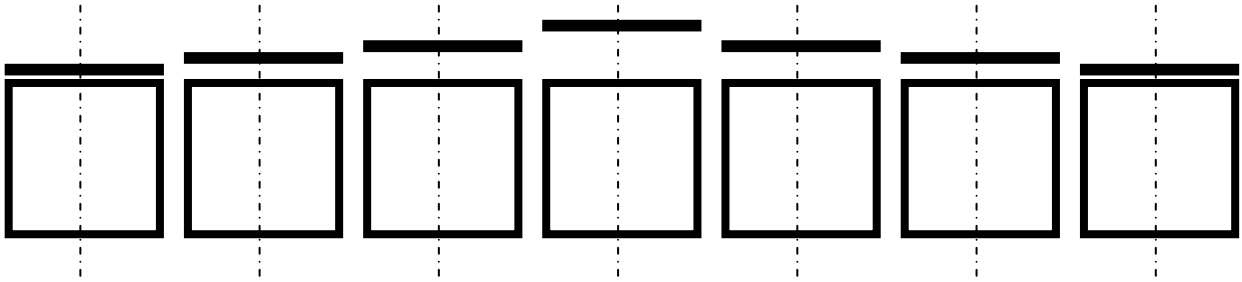

Figure 6 – *PRV* schematic process, with different valve openings as a function of time

3. RESULTS

In order to compare the discharge coefficient obtained using the two different approaches, a test case was carried out and the results were analyzed. The set point pressure and the operation pressure were defined as P_{sp} = 2 kgf/cm^2(a) and P_a = 2.5 kgf/cm^2(a). The spring dimensional parameters were specified as: k = 4 kgf/mm and c = 15 kgf-s/m; additionally for the disc mass was established a m_D = 200 g. For this condition, the initial spring deformation Y_o is 18.5 mm, with a natural frequency of 443 rad/s and a damping ratio of 0.8. The last parameter determines that the system would have an under-damped behavior (Inman, 2000).

Figure 7 shows the *PRV* disc displacement as a function of time obtained via the two approaches. It can be seen that during the transient state, the one-dimensional approach (1-D) presented an abrupt lift of the valve disc; on the other hand, the two-dimensional approach (2-D) showed a more damped displacement of the valve disc. A significant difference was obtained for the final equilibrium disc position. The 2-D approach showed an equilibrium valve disc displacement of almost 50% of the 1-D approach (13mm), indicating that the flow curvature induced smaller fluid force on the valve disc.

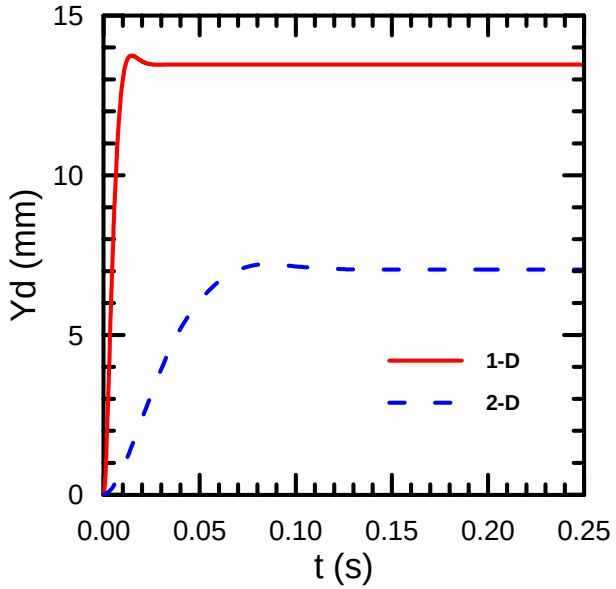

Figure 7 – *PRV* disc displacement through the time

Figure 8 shows the time variation of the outlet flow rate through the *PRV* obtained by the two approaches. In agreement with the valve disc displacement presented, the 1-D approach showed a sudden increasing of the output flow. Similarly, the 2-D approach presented a more damping behavior. As a consequence of the smaller steady state valve opening, the 2-D approach showed an equilibrium flow rate approximately 40 % smaller than the equilibrium flow rate obtained with the 1-D approach.

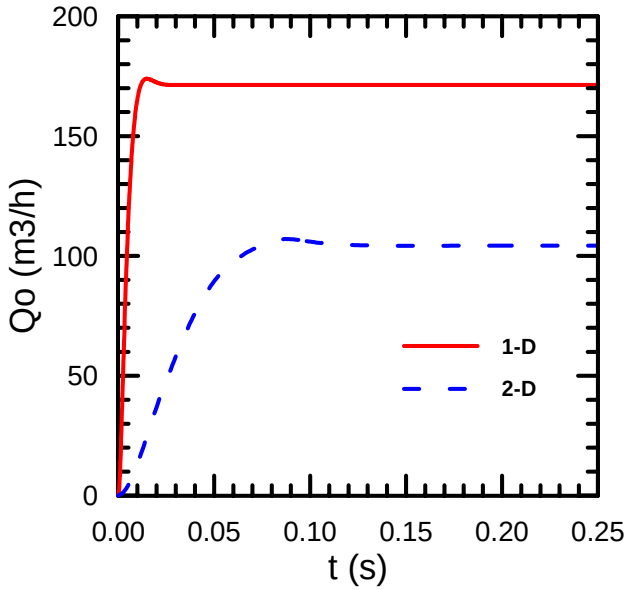

Figure 8 – *PRV* output flow rate through the time

As the valve opened by the disc displacement, the velocity at the inlet increased. Once the total pressure was kept constant at the valve inlet, the inlet static pressure was reduced in order to relieve the operation pressure. The Figure 9 presents the inlet static pressure obtained by the two approaches, where it can be seen that, as expected, the predictions for the inlet static pressure showed an analogous behavior as the flow rate. The fast increase of the flow rate of the 1D model induced an abrupt pressure drop, due to the large dynamic pressure. On the other hand, the 2-D approach presented a smooth drop of the static pressure. Figure 9 also illustrates the static pressure at the valve disc bottom, where it can be clearly seen a pressure oscillation as the valve disc opens, due to the flow adaptation to the new geometry, with smaller flow curvature in direction to the valve exit. As the valve disc reaches an equilibrium position, the valve disc pressure stabilizes. Note also that, as expected, the valve disc pressure is smaller than the inlet static pressure.

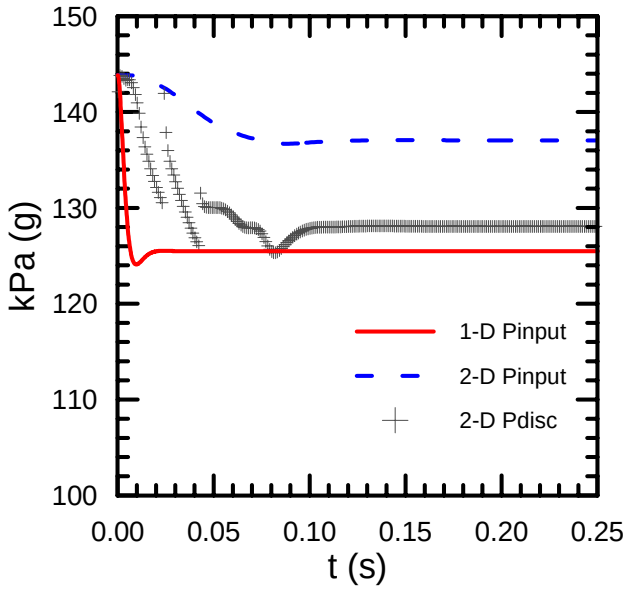

Figure 9 – Static pressure in the *PRV* input and in the *PRV* disc bottom through the time

Figure 10 presents the discharge coefficient C_d variation along time obtained by means of the two approaches. Note that as a consequence of the larger valve disc displacement of the 1-D approach in relation to the 2-D approach, this situation originated a higher discharge coefficient for the first one.

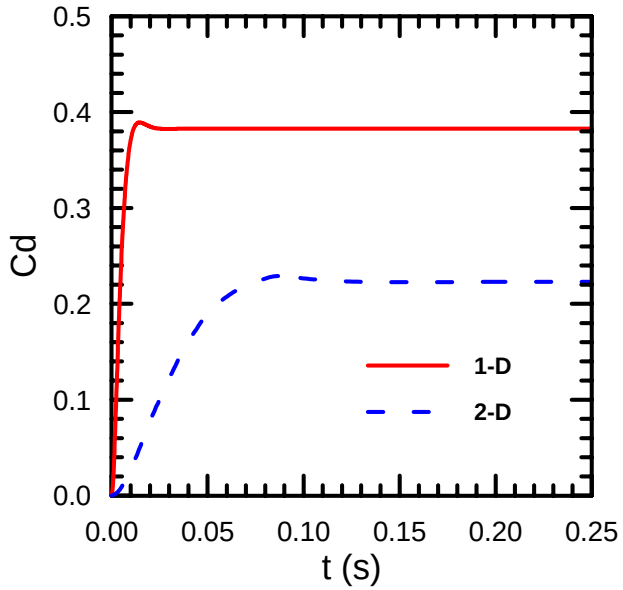

Figure 10 – *PRV* discharge coefficient through the time

Figure 11 illustrates the discharge-coefficient as a function of the normalized valve opening (ratio of disc displacement to the maximum opening), as commonly informed by the valve manufactures. Note that in spite of the distinct results obtained using both approaches, the discharge coefficient C_d versus normalized valve-opening coincides perfectly. This is an excellent result which meaning that in practical situations the simplified 1-D model can be successfully coupled inside a pipeline network simulator, expecting a correct discharge coefficient behavior. Further, this last result implies that the steady state flow procedure is valid to calculate this critical parameter.

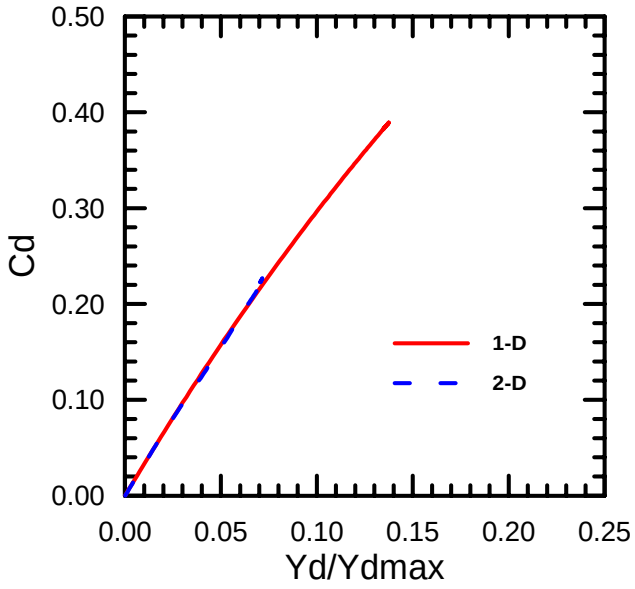

Figure 11 – *PRV* discharge coefficient for different valve disc positions

5. FINAL REMARKS

In the present work a two-dimensional transient analysis of the flow inside a direct acting spring loaded pressure relief valve has been performed, aiming the determination of the discharge coefficient C_d by a more accurate methodology, considering the valve dynamic behavior.

The results were compared against these obtained with a one-dimensional integral model. The results showed that although different valve disc equilibrium positions and flow rates were obtained by each approach, both models predicted the same behavior for the discharge-coefficient as a function of the normalized valve aperture.

To support these results and conclusion, additional more complex cases, with more realistic *PRV* designs and

different operational conditions are being examined. Further, a test facility is being constructed to adjust and calibrate the valve parameters.

6. ACKNOWLEDGEMENTS

The authors thank FINEP and CNPq for supporting the development of this work.

7. REFERENCES

Boccardi, G., Bubbico, R., Celata, G.P. and Mazzarotta, B., 2005, “Two-Phase Flow Through Pressure Safety Valves – Experimental Investigation and Model Prediction“, Chemical Engineering Science Vol. 60, pp. 5284-5293.

Catalini, L., 1984, “Dynamic stability analysis of spring loaded safety valves – Elements for improved valves performance through assistance devices”. Conference on Structural Mechanical in Reactors, August 22-26.

Dasgupta, K. and Karmakar, R., 2002, “Modelling and dynamic of single-stage pressure relief valve with directional damping”, Simulation Modelling Practice, Vol. 10, pp. 51-57.

Fluent Users Guide, 2008, Fluent Inc.

Inman, D.J., 2000, “Engineering Vibration”, Prentice Hall, 2th edition.

Launder, B. E. and Spalding, D. B., 1974, "The numerical computation of turbulent flows", Computer Methods in Applied Mechanics and Engineering, Vol. 3(2), pp. 269-289.

MacLeod, G., 1985, “Safety valve dynamic instability: an analysis of chatter”, ASME Journal of Pressure Vessel Technology, Vol. 107, pp. 172-177.

Maiti, R., Saha, R. and Watton, J., 2002, “The static and dynamic characteristics of a pressure relief valve with a proportional solenoid-controlled pilot stage”, Proc Instn Mech Engrs, Vol. 216, Part I, pp 143-156.

Menter, F. R., 1994, “Two-Equation Eddy-Viscosity Turbulence Models for Engineering Applications”, AIAA Jounal, Vol. 32, No. 8, pp. 1598-1605.

Ortega, A.J., Pires, L.F.G. and Nieckele, A.O., 2008a, “Numerical Simulation of Incompressible Flow through a Pressure Relief Valve”, 5th National Congress of Mechanical Engineering, CONEM, Salvador, BA.

Ortega, A.J., Azevedo, B.N., Pires, L.F.G., Nieckele, A.O. and Azevedo, L.F.A., 2008b, “A Numerical Model about The Dynamic Behaviour of a Pressure Relief Valve”, 12th Brazilian Congress of Thermal Engineering and Sciences, Belo Horizonte, MG.

Shin, Y.C., 1991, “Static and Dynamic Characteristics of a Two Stage Pilot Relief Valve”, Journal of Dynamic Systems, Measurement, and Control, Vol. 113, pp. 280-288.

8. RESPONSIBILITY NOTICE

The authors are the only responsible for the printed material included in this paper.